

MET.O.14

METEOROLOGICAL OFFICE
BOUNDARY LAYER RESEARCH BRANCH
TURBULENCE & DIFFUSION NOTE



T.D.N. No. 116

Spectral characteristics of surface layer turbulence

over the sea

by

S.Nicholls & C.J.Readings

January 1980

Please note: Permission to quote from this unpublished note should be obtained from the Head of Met.O.14, Bracknell, Berks., U.K.

FH13

Spectral characteristics of surface layer
turbulence over the sea.

S Nicholls
and
C J Readings

NOTATION

Co_{xy}	cospectrum of parameters x and y
f	non-dimensional frequency = nz/U where U is the airspeed relative to the instrument platform. f_1 and f_2 refer to alongwind and acrosswind sampling directions respectively.
f_d	= z/λ_d
g	acceleration due to gravity
k	von-Karman constant (= 0.4)
L	Monin-Obukhov length = $-u_*^3 \bar{T}_V / (gk (\bar{w}\bar{T} + 0.61 \bar{T} \bar{w}q))$
n	frequency (Hz)
N_T, N_q	rates of dissipation of temperature and humidity variance ($\bar{T}^2/z, \bar{q}^2/z$) respectively
q	Humidity mixing ratio
S_x	spectrum of parameter x
T	temperature
T_V	virtual temperature
u	alongwind air velocity component
v	acrosswind air velocity component
w	vertical air velocity component
z	height above sea surface
\hat{z}	= $-z/L$
z_i	height of lowest inversion base
α, β_T, β_q	Kolmogorov constants for velocity, temperature and humidity spectra (taken as 0.5, 0.9 and 0.8 respectively)
ϵ	rate of dissipation of kinetic energy. Denoted ϵ_x when calculated from the S_x .
ϕ_ϵ	dimensionless dissipation rate for velocity fluctuations = $\epsilon z/u_*^3$

ϕ_q	dimensionless dissipation rate for humidity fluctuations $= N_q z/u_* q_*^2$
ϕ_T	dimensionless dissipation rate for temperature fluctuations $= N_T z/u_* T_*^2$
σ_x	standard deviation of parameter x
$\lambda_m(x)$	wavelength at which the spectral peak of parameter x occurs. Alongwind and acrosswind sampled values denoted λ_{1m} , λ_{2m} respectively.
λ_d	dominant acrosswind sampled wavelength (see text)
τ_o	surface stress

Surface scaling parameters u_* , T_* and q_* are calculated from surface flux values obtained by extrapolation from aircraft measurements (see Nicholls and Readings, 1979).

Alongwind and acrosswind sampling is denoted by (n,o,o) and (o,n,o) respectively.

An overbar represents an average taken over the duration of one flight leg (approximately 60 km in most cases).

ABSTRACT

Airborne measurements of atmospheric turbulence spectra and cospectra made at low levels in convective boundary layers over the sea around the UK are presented. Both alongwind and acrosswind sampled data are considered. In general, the former agree well with the results of other workers obtained over the sea using surface based instrumentation, though the forms of their temperature spectra vary widely. The present alongwind data are also compared with corresponding results obtained over land. Again the velocity spectra agree closely but the temperature spectra differ appreciably.

Both along and acrosswind spectra vary with stability, increases in convective activity being associated with increased energy at low frequencies. No corresponding change was observed in the cospectra.

A comparison of along and acrosswind sampled spectra and cospectra reveals considerable differences. These are consistent with a redistribution of energy from high to low frequencies on changing from acrosswind to alongwind sampling. Thus the acrosswind spectra and cospectra appear more narrow (by about one decade). Spectral and cospectral peaks are also shifted. These observations are consistent with the stretching effects of the mean velocity shear acting on convective elements.

The dissipation parameters derived from the high frequency parts of the spectra appear quite reasonable though there is a systematic difference between those derived from vertical and horizontal velocity spectra.

1. Introduction

During 1975 and 1976, the Hercules aircraft belonging to the Meteorological Research Flight made a series of eight flights over the sea surrounding the UK in order to investigate the structure of the marine* boundary layer. The measured fluxes and variances together with details of the overall thermodynamic structure have already been published (Nicholls & Readings, 1979). The present paper extends this work by presenting the results of a spectral analysis, again concentrating on the lower parts of the boundary layer where effects due to variations in cloud dynamics and entrainment should be at a minimum.

A novel feature of the data presented in this paper is that the measurements were made in both the streamwise (alongwind) and transverse (acrosswind) directions. Most previous measurements (eg. Kaimal et al (1976), Phelps et al (1971), Leavitt (1975)) have been made from fixed points (eg. tethered balloons, towers or ships) where only streamwise measurements are possible. Very few measurements of spectra in the atmospheric boundary layer have been made in any direction other than alongwind. Furthermore, those that have been published (eg. Warner (1973), Nicholls (1978)) have not been analysed in any systematic manner. In the present paper, comparisons are made between both these sets of measurements as well as between the alongwind data and previous work over both land and sea.

2. The Data

The data used in this analysis have been taken from the set reported by Nicholls and Readings (1979). This covered a wide range

* Throughout this paper 'marine' refers to the atmosphere over the sea rather than the actual structure of the sea.

TABLE 1

Date	No of spectra	U_{*1} ms ⁻¹	T_{*} °C	q_{*} $\times 10^{-3}$	-L m	$-z_i/L$	measurement heights m
26/2/75	4	0.41	0.037	0.032	280	1.3	30, 30, 90, 90
2/4/75	4	0.45	0.011	-	1300*	0.5	60, 60, 120, 120
10/9/75	2	0.30	0.050	0.170	82	7.3	65, 140
10/9/75	2	0.34	0.044	0.150	120	5.0	65, 140
15/9/75	4	0.40	0.045	0.078	195	2.3	40, 45, 95, 95
23/9/75	3	0.66	0.041	0.026	635	0.6	40, 95, 100
28/1/76	6	0.62	0.022	0.017	1090	0.9	90, 90, 95, 95, 160, 165
21/1/76	2	1.06	0.053	0.064	1250	1.6	220, 230
13/2/76	1	0.45	0.046	0.051	260	3.3	35
13/2/76	4	0.40	0.047	0.048	205	4.1	35, 40, 95, 95

* Surface moisture flux assumed zero.

of meteorological conditions ranging from a fully suppressed, cloudfree situation to a severe gale although in each case the boundary layer was convectively unstable (the sea surface being warmer than the air).

The data are biased towards higher windspeed conditions and most of the flight levels placed in the lower parts of the mixed layer. Full details are contained in Nicholls & Readings (1979), but some relevant information taken from that paper is reproduced in Table 1.

The present paper concentrates on data obtained on the lowest runs ($z < 0.25z_1$), the heights ranging from 30m to 200m. The measurements are grouped according to the direction of sampling: either acrosswind or alongwind since there are significant differences in their spectral characteristics. However as the fluxes and variances do not in general show any dependence on sampling direction (Nicholls and Readings, loc cit), the same surface layer parameters are used to scale both sets of spectra (see Section 3).

Corrections have been applied to overcome the limitations in the response characteristics of the temperature and humidity sensors (Nicholls, 1978). In addition, high frequency noise has been removed from the velocity components (ibid) which are referred to a right-handed co-ordinate system in which the u-component is parallel to the mean wind direction (as defined in Nicholls & Readings, loc cit.)

Recently many of the temperature measurements made over the sea have been questioned (Schmitt et al, 1978) because the time series contain unusual characteristics ('cold spikes') which are difficult to explain in terms of any physically realistic model. Well defined 'inertial subrange' behaviour, present in all other parameters, is also absent in these temperature spectra. The problem appears to be caused by salt contamination of the thermometer resistance wire since the

hygroscopic nature of the salt residue induces a sensitivity to humidity fluctuations (Schmitt et al, loc cit). Although similar features have been observed in aircraft results in very moist conditions (near cloudbase over tropical oceans, Nicholls & LeMone (1979)), no such behaviour is apparent in the present data. The relatively low humidity mixing ratios encountered here together with the temperature rise in the airborne thermometer due to adiabatic compression appear to combine to produce too low a relative humidity in the thermometer housing for this effect to occur. Further support for the view is provided by the estimates of temperature fluctuation dissipation rates derived from the spectra which are approximately in balance with the predicted production term (see Section 7). Furthermore, the value of the sensible heat transfer coefficient obtained by Nicholls & Readings (loc cit) is in close agreement with other (uncontaminated) measurements.

The spectra and cospectra were computed using a fast Fourier transform algorithm and averaged over eight frequency bands per decade where the density of spectral estimates permitted.

3. The Analysis Scheme

In the stability range covered by this data set ($0 < -z_1/L < 10$), the turbulence structure remains sensitive to τ_0 , the surface stress, to much greater heights than is the case for a more vigorously convectively mixed layer over land ($-\frac{z_1}{L} \sim 100$), (see discussion in Nicholls & Readings, 1979). Two idealized situations may be envisaged:

- (1) $-z_1/L \gg 10$ (typical of convective conditions over land).

Here there are two main regions. Firstly, a 'surface' layer extending to a height of about $0.1z_1$ (where Monin-Obukhov similarity is valid) above which lies the 'mixed' layer (see, for example Kaimal et al, 1976). Between these two there may also be a matching or 'free convection layer' (eg. Panofsky, 1978).

(ii) $-z_1/L < 10$ (present data). Above the surface layer there is now a region where neither surface layer nor mixed layer scaling is valid since the turbulence remains sensitive to both T_0 and z_1 (Nicholls and Readings, loc cit). The height at which surface layer scaling breaks down is uncertain, but probably $\sim 0.25z_1$ (see below). Mixed layer scaling may be valid at still higher levels depending on the values of z_1 and L .

However, this simple picture is complicated by the behaviour of the horizontal wind components. Thus, for example, at low frequencies in very unstable conditions Kaimal (1978) found that his horizontal velocity spectra showed a dependence upon z_1 even within the surface layer ($z < 0.1z_1$). Panofsky et al (1978) have also presented data supporting this view. Clearly the optimum choice of scaling for spectra remains debatable although it is unlikely that any one simple method can consistently provide 'universal' scaling for all the parameters considered here even near the surface.

Given this uncertainty, the data included in the present analysis were selected from only the lowest flight levels ($z < 0.25z_1$). Here any effects associated with a z_1 dependence should be at a minimum, if not altogether negligible. The data were therefore scaled with the surface layer scheme which, with documented exceptions, appears to succeed fairly well in ordering the individual spectra.

This choice is supported by the behaviour of the wavelengths at which spectral peaks (λ_m) of a number of parameters are located. These are found to vary approximately linearly with z (see Section 4a). Furthermore there is good overall agreement between spectra and cospectra normalised in this way with corresponding results derived from other surface layer measurements (see Section 4).

The data were therefore grouped according to values of $\hat{z}(=z/L)$. Runs for which $\hat{z} > 0.15$ were allocated to Class I with the more stable conditions ($\hat{z} < 0.15$) falling into Class II. The actual value of \hat{z} chosen to delineate the classes is not crucial provided each contains sufficient data for meaningful averages to be formed and the two classes are sufficiently different for any stability effects to be apparent. It is not practical to subdivide further given the limited range of stability covered by the data. There are 21 runs in Class I and 11 in Class II. The mean value of \hat{z} for Class I is 0.45, while for Class II it is 0.10. Individual values lie in the range $0.05 < \hat{z} < 1.3$. Since the spectra are discussed mainly in terms of class mean values, Fig 1 shows a typical example of the scatter and the separation of individual points into the two classes. The choice of coordinates and scaling are discussed below.

Following Kaimal et al (1972), the spectral density in the inertial subrange of a velocity component x may be expressed as

$$\frac{nS_x(n,0,0)}{u_*^2 \phi_\epsilon^{2/3}} = \frac{\alpha}{(2\pi)^{2/3}} f^{-2/3} \quad (1)$$

where $\phi_\epsilon (= \epsilon z / u_*^3)$ is the dimensionless dissipation rate for velocity fluctuations and α is the Kolmogorov constant (a factor of $4/3$ is also involved if the sampling direction is normal to the velocity component, x). Since this expression is a function of f only, normalisation of the spectra using u_* and ϕ_ϵ should collapse each one onto a single curve at high frequencies (when plotted against f), though stability effects (different values of \hat{z}) may make them diverge at low frequencies.

However, as no direct measurements of ϵ (and therefore of ϕ_ϵ) are available, each spectrum was individually fitted by a least squares method to a ' $-2/3$ rds' power law in the frequency interval $1 < f < 10$. Full account was taken of the small deviations from this behaviour (near $f = 1$)

noted by Kaimal et al (1972) though this only marginally affects the results. The scaled spectra are thus directly comparable with those published by Kaimal et al (loc cit) which have been superimposed on the alongwind sampled spectra presented below. The implied values of ϵ are discussed in Section 7.

Equations similar to (1) can be written for temperature and humidity spectra:

$$\frac{nS_T(n,0,0)}{T_*^2 \phi_T \phi_\epsilon^{-1/3}} = \frac{\beta_T}{(2\pi)^{2/3}} f^{-2/3} \quad (2)$$

and

$$\frac{nS_q(n,0,0)}{q_*^2 \phi_q \phi_\epsilon^{-1/3}} = \frac{\beta_q}{(2\pi)^{2/3}} f^{-2/3} \quad (3)$$

where ϕ_T and ϕ_q are dimensionless dissipation rates for temperature and humidity (see notation for definitions). Acrosswind sampled spectra are treated in an identical manner.

The cospectra (multiplied by frequency ie $nCo_{xy}(n)$) have been normalised by the surface scaling parameters (see Table 1) and plotted against f . The areas enclosed by these curves are then proportional to the covariance. Class distinctions are ignored in presenting these cospectra because no significant differences could be detected (except for two minor exceptions discussed in section 5c).

4. Alongwind measurements

(a) Velocity Spectra

Fig 2 shows the alongwind sampled velocity spectra with the data divided into the two classes. At high frequencies, each of the spectra display about one decade of ' $-2/3$ rds' power law behaviour although the u-spectra show some signs of contamination for $f > 2.0$ (see Nicholls, 1979). Class I and Class II data differ appreciably, spectra from more unstable conditions showing a marked increase in energy at low frequencies.

This is especially true of the horizontal velocity spectra. Here the proximity of the surface ensures that any increase in convective activity is mainly observed as an increase in the low frequency energy of the horizontal velocity components. However, this large increase in energy does not appear to significantly affect momentum transfer at low frequencies (see 4c below). Such induced motion has been called the 'inactive motion' by Bradshaw (1978) and is clearly the main cause of the marked changes in σ_v (and also σ_u) with stability noted in an earlier paper (Nicholls and Readings, 1979). The curves drawn on the figure represent the results of the Kansas experiment (Kaimal et al 1972)) which are generally accepted as a standard for surface layer measurements over land. The three curves on the w-spectra correspond to specific values of \hat{z} while the lines on the other two velocity spectra represent the limits of the unstable Kansas data ($0.0 < \hat{z} < 2.0$) in which no systematic variation with \hat{z} was observed. However, a subsequent analysis of surface layer spectra by Kaimal (1978) showed that the low frequency part of the horizontal velocity spectra scaled with the boundary layer height, z_i , while Monin-Obukhov scaling was applicable to the higher frequencies. Such behaviour is also found in laboratory flows (Bradshaw loc cit) where the 'inactive' motion also scales with mixed layer depth. Thus the differences between the two sets of horizontal velocity spectra in Fig 2 may reflect changes in z_i/L rather than \hat{z} . Unfortunately it is not possible to resolve this question with the present data since grouping the results according to values of z_i/L produces virtually the same distribution as the present classification. More data is required to test this hypothesis.

In near neutral conditions (ie Class II), the v-component has much less energy at low frequencies than either the corresponding u-spectrum or the Kansas results. In fact the Class II v-spectrum is not unlike the

Class II w-spectrum having a spectral peak at $f_1 \approx 0.2$. Under more unstable conditions, the two horizontal components contain approximately the same amount of energy at low frequencies while the vertical component has little energy in this part of the spectrum demonstrating the two-dimensional nature of atmospheric motion on these scales. There is still a suggestion of a peak at $f_1 \approx 0.2$ in the more unstable (Class I) data. Indications of a change in character of both the u and v spectra at $f_1 \approx 0.2$ were noted by Kaimal et al (1972) although the effect was less marked than is found here.

The positions of the peaks of individual vertical velocity spectra ($\lambda_m(w)$) are plotted as a function of height in Fig 3 (both along and acrosswind measurements are included since no significant change between $\lambda_{1m}(w)$ and $\lambda_{2m}(w)$ could be detected). Despite the scatter, $\lambda_m(w)$ is seen to vary approximately linearly with height suggesting that the data is scaled well by the surface layer scheme. The dashed lines on the figure represent the expected variation of the non-dimensional peak frequency, $f_{1m}(w) = z/\lambda_{1m}(w)$, from the Kansas results across the stability range encompassed by the present data. Although the stability range is small, Fig 2 does show a tendency for $f_{1m}(w)$ to decrease with increasing instability in agreement with the Kansas data.

Spectra obtained over the sea by other workers are summarized in Fig 4. As individual authors have generally employed different methods of scaling, it is only possible to compare the overall spectral shapes. Data from the sources detailed in the legend have been combined and envelopes containing approximately 95% of the points are defined by the shaded regions. Parts of spectra that are clearly erroneous (eg. due to sensor motion) have been omitted.

The data available for comparison have generally been obtained in fairly unstable conditions, consequently more than 95% of these data

fall into the 'class I' group. Comparisons are therefore only valid for the more unstable case. With this restriction, the velocity spectra are seen to lie well within the range of previously reported marine surface layer data.

(b) Temperature and humidity spectra

The alongwind sampled temperature spectra are shown in Fig 5 with the curves again representing the envelope of the unstable Kansas data ($0 \leq z \leq 2.0$). There appears to be a reasonable approach to a ' $-2/3$ ' dependence at high frequencies although the band is rather narrow and is the least well defined of any of the spectra. The spectra are clearly bimodal with one high frequency peak near $f_1 \sim 0.6$ and a second at lower frequencies. The energy associated with the latter again increases with increasing instability.

These spectra are clearly very different from those measured over land in similar conditions reflecting major differences in temperature structure.

The results of Donelan & Miyake (1973) and Phelps & Pond (1971, San Diego data) also obtained at low levels over the sea in unstable conditions (see Fig 5b) show a similar bimodal shape with a high frequency peak near $f_1 \sim 0.6$. Measurements of temperature spectra by Leavitt (1975) and Phelps and Pond (loc cit) made during BOMEX (Barbados Oceanographic and Meteorological Experiment) are also reproduced in Fig 5b although both are suspected to have been significantly affected by the contamination problem discussed in section 2.

The Kansas temperature spectra resemble more the humidity spectra obtained over the sea (see Fig 6a). This may reflect the structure of the lowest few metres of the convective boundary layer where large gradients often exist. Over land there is typically a large temperature

gradient while over the sea a large humidity gradient is found. Thus a fluid particle displaced upwards from a position near the sea surface might be expected to retain its identity longer when defined in terms of q rather than T since the air-surface difference is relatively large compared to local fluctuation levels at measurement height. e.g. over the sea $\Delta \bar{q} / \sigma_q \approx 17$, $\Delta \bar{T} / \sigma_T \approx 7$ (where Δ refers to a surface -10m difference). Therefore, the characteristic 'top-hat' temperature trace associated with updraughts over land (e.g. Lenschow, 1970) is replaced over the sea by a characteristic humidity increase (and a corresponding decrease in u). Thus similarities between the q - (and u -) spectra over water and the T -spectra over land are not altogether unexpected.

The humidity spectra are compared with previous measurements made over the sea in Fig 6b.

(c) Cospectra

The mean cospectra are shown in Fig 7 with data from classes I and II combined (see section 4). Measurements by Leavitt (1975) are included for comparison.

Almost 20% of the total uw - and wq - covariance lies in the band $10^{-3} < f_1 < 10^{-2}$ (5% for wT). Thus the spectral range of eddy correlation measurements must extend to at least $f_1 = 10^{-3}$ if the fluxes are not to be seriously underestimated. The fraction of the covariance contained in this band does not appear to change significantly between classes I and II despite the large increases in spectral density observed at low frequencies in u and q (see section 4a).

The uw - and wq - cospectra both agree very closely with those published by Leavitt (loc cit) and both peak at $f_1 = 0.035$. The wT -cospectrum is relatively smooth having a broad maximum, reflecting the behaviour of the vertical velocity and temperature spectra: the peak of the former lying between the double maximum of the latter. It is

possible that this difference in cospectral shape is related to the different height range at which these data were collected since the wT -cospectra do seem to be more sensitive to the height above the surface than other cospectra (see also the acrosswind results). The higher frequency peak in the temperature spectra and a corresponding peak in the \overline{wT} -cospectra might only be dominant at the very low levels accessible to surface based observations. The magnitude of \overline{wT} certainly falls off more quickly with height than either \overline{wq} or \overline{uw} (Nicholls and Readings, 1979) as is evident in the figure, where the area under the scaled MRF \overline{wT} cospectrum (proportional to the covariance in this presentation) is rather less than that enclosed by Leavitt's data which were obtained at lower levels ($z \leq 30m$). This decrease in \overline{wT} appears to be solely due to a decrease in cospectral density at higher frequencies ($f_1 > 0.1$) although Leavitt's near surface results have been questioned because of possible contamination effects.

Fig 8 shows comparisons with previously reported measurements made over the sea together with an indication of the scatter present in the individual cospectral estimates.

(d) The Validity of Taylor's hypothesis

With the possible exception of the T-spectra and \overline{wT} -cospectrum, the degree of correspondence between the aircraft results and previous measurements is clearly very good. Most of the comparison data were obtained from fixed point measurements, where the transformation to wavenumber spectra is achieved by use of Taylor's hypothesis (eg. Kaimal et al, 1972). This has often been criticised on the grounds that the application of a 'frozen-field' hypothesis might seriously distort one-dimensional wavenumber spectra measured from a fixed point (especially at small wavenumbers). The degree of agreement found here between the aircraft and fixed point measurements does not readily support such a view.

5. Acrosswind measurements

In presenting these results, some differences between across and alongwind sampled measurements are mentioned, but a more comprehensive discussion is deferred until section 6.

(a) Velocity spectra

The acrosswind sampled velocity spectra are shown in Fig 9. As in the alongwind case, the spectra show well-marked ' $-2/3$ ' regions and large increases in low frequency energy with increased instability. The peaks of the w-spectra occur at the same reduced frequency as the alongwind data (see Fig 3), the w-spectra being very similar to the low level acrosswind measurements made by Warner (1973).

The most notable feature of the acrosswind sampled data is the presence of a well defined peak in S_u for both Classes at $f_2 \approx 0.2$. The location of this feature is scaled fairly well by the surface layer scheme (as shown by Fig 10). The Class II v-spectrum also has a peak at $f_2 \approx 0.2$ as in the alongwind case.

(b) Temperature and humidity spectra

The temperature spectra shown in Fig 11 have the same characteristic shape as was observed alongwind although the energy associated with the high frequency maximum is now comparable in magnitude to that at lower frequencies. This mainly reflects a decrease in spectral energy at low frequencies relative to that at higher frequencies, a common feature of acrosswind sampled spectra. The high frequency maximum is more clearly defined acrosswind and shifts to a lower frequency in the more unstable case. The maximum occurs at the same value of f_2 as the vertical velocity maximum (see Fig 9).

The humidity spectra are again similar to the u-spectra, as was the case alongwind, with a pronounced peak near $f_2 \approx 0.15$.

(c) Cospectra

The scaled cospectra formed from all acrosswind measurements are shown in Fig 12. The bandwidth of significant contributions to the covariance is about one decade less than that measured alongwind due to the decreased cospectral density at lower frequencies, a trend which was also noticed in the power spectra. The acrosswind cospectra are therefore narrower than their alongwind counterparts, the peaks occurring at approximately the same reduced frequency in each case ($f_2 \sim 0.2$).

Small but distinct changes were observed in both the uw- and wT- cospectra associated with variations in stability. These are illustrated by the shading in Fig 12. Under more unstable conditions the peak of the uw- cospectrum increases in size without shifting along the f_2 axis. There is also a tendency for uw cospectral estimates to reverse sign near $f_2 \sim 0.01$. It is interesting to note that both of these findings were predicted by Straka et al (1978) using a semi-empirical theoretical approach. This sign reversal, observed in many of the more unstable cases, suggests that larger scale motions associated with convection can transport momentum against the local velocity gradient. Similar tendencies have been reported by other workers using fixed point measurements (eg. Kaimal et al (1972), Pond et al (1971), Zubkovskij and Koprov (1969)) although the sign reversals occur at lower frequencies ($f < 0.01$) in these 'alongwind' sampled results where cospectral estimates are usually very erratic. Thus no clear demonstration of this behaviour has emerged.

The wT- cospectra also show a tendency to reverse sign at lower frequencies, the effect becoming more noticeable with increasing height (see Fig 12). In fact the acrosswind wT- cospectra do not appear to be particularly well scaled by surface layer methods; not only do the shapes of the cospectra change with height, but the position of the

peaks tend to occur at the same dimensional frequency. Thus scaling with z tends to separate the peaks slightly and leads to a slightly skewed envelope (see Fig 12).

6. Comparison of along and acrosswind results

A number of changes have been shown to occur in both spectra and cospectra as stability and sampling direction are varied. These are now examined in detail and the physical implications considered.

Turning first to the variations in spectra with sampling direction, Fig 13 shows how the ratios of the acrosswind to corresponding alongwind sampled spectral densities vary with dimensionless wavenumber. With the exception of v , the curves are very similar despite the large variability in spectral shapes shown earlier. There is consistently more energy in the acrosswind sampled spectra at $f \sim 0.2$ and more in the alongwind sampled spectra at $f < 0.1$. Changing stability seems to make little difference to this behaviour. Thus a marked redistribution in spectral energy occurs in each of the u , w , \bar{T} and q spectra between the along and acrosswind measurements. Similar behaviour is also apparent in the cospectra shown in Fig 14 where the acrosswind peak at $f \sim 0.2$ is shifted to smaller values of f in the alongwind case with a corresponding increase in cospectral energy at low frequencies.

The most satisfactory interpretation of this behaviour is that 'u-eddies' are stretched by the mean wind shear, which is virtually parallel to the mean wind direction (see Nicholls and Readings, 1979), such that they become elongated in the alongwind direction. Thus a fluid particle displaced, say, upwards will become stretched in the u -direction and since temperature and humidity fluctuations are also correlated with those of u (through the action of w), the spectra of these variables will also show similar behaviour. This may be contrasted

with the behaviour of the v - spectra which are not appreciably different along either sampling direction, v fluctuations not being strongly correlated with fluctuations in either u or w . The maximum spectral energy loss from the acrosswind to the alongwind spectra occurs at the same nondimensional frequency ($f \approx 0.2$) as the acrosswind uw -copspectral peak, which is by definition the frequency at which u and w are best correlated.

Each of the alongwind sampled spectra might therefore be interpreted as a distorted counterpart of the corresponding acrosswind sampled spectrum where energy has been shifted to smaller wavenumbers by the stretching action of the mean shear. Deardorff (1972) drew similar conclusions in interpreting the results of his numerical simulations.

Changing stability seems to have little effect on this re-distribution of energy, for despite the large changes in low frequency spectral density (especially u, v , and q) associated with variation in stability, the ratios shown in Fig 13 remain largely unaltered.

In similar conditions other workers (eg. LeMone, 1973) have reported the presence of horizontal roll vortices, one of whose characteristics is the distortion of across and alongwind spectra in a manner similar to that observed above. It is interesting to speculate on the relationship between roll spacing and the dominant acrosswind wavenumber f_d ($= \frac{z}{\lambda_d} = 0.2$) observed here by estimating the likely range of values of λ_d in the middle of the mixed layer.

Previous results (eg. Kaimal et al, 1976) have shown that surface layer scaling (with z) fails above a certain value of z/z_1 , above which λ_d appears to be almost constant until a height of about $0.8z_1$ is reached where the effects of mixing at the inversion interface become important. Since the present results show that

surface layer scaling appears to be satisfactory to at least $0.25z_1$, the range of possible λ_d in the rest of the mixed layer is

$$\frac{0.25}{0.2} z_1 < \lambda_d (= z/f_d) < \frac{0.8}{0.2} z_1$$

$$\text{or } 1.25 z_1 < \lambda_d < 4 z_1$$

which includes the generally accepted range of values for roll spacing of $1.5z_1 - 3.5z_1$ (LeMone, 1973). Thus horizontal roll vortices can give rise to similar spectral characteristics as those documented above in the middle of the mixed layer. However, it seems unlikely that these provide an explanation of the changes observed here.

All the measurements were made at low levels ($z < 0.25z_1$) where surface layer scaling orders the spectra reasonably well. Horizontal rolls would be expected to scale with z_1 and not z . Rolls also tend to have a very narrow spectral signature and although narrow spectral peaks which did not scale with z were observed on some flights (eg. Nicholls, 1978), the bulk of the individual spectra and cospectra, including those containing narrow peaks, behaved in the manner described above where changes are observed over broad frequency bands. Organisation of cumulus cloud near the top of the mixed layer into bands orientated alongwind was observed on only two occasions. However, the elongation of eddies by shear and the presence of secondary flows might be interactive and complementary. Only further study throughout a greater depth of the boundary layer will clarify the situation.

7. Dissipation estimates

The method of scaling the spectra employed earlier (see section 3) was to fit the high frequency parts of the spectra (where a $-2/3$ power law was evident) to semi-empirical curves (ie. equations 1, 2 and 3). This procedure was necessitated by the lack of direct measurements

of the dissipation parameters ϵ , N_T or N_q . However, this matching does enable these parameters to be estimated if the Kolmogorov constants α , β_T and β_q are specified.

Values of ϵ were calculated from each of the individual u , v and w spectra from each run (called ϵ_u , ϵ_v and ϵ_w respectively). These estimates are compared in Fig 15. With perfect instrumentation and isotropic turbulence in the frequency band over which the spectra were matched to the curves, then $\epsilon_u = \epsilon_v = \epsilon_w$. However, it is clear from Fig 15 that ϵ_w tends to be systematically smaller ($\sim 30\%$) than either ϵ_u or ϵ_v which are roughly equal. The mean ratio of the vertical to the longitudinal power spectrum is found to be 1.07 rather than 1.33 expected in an inertial subrange. Other workers have reported similar values over the sea (Weiler and Burling (1967), Donelan and Miyake (1973)) although Kaimal et al (1972) showed that the ratio does attain the expected value over land if the observations extend to sufficiently high frequencies ($f \gtrsim 3$ for near neutral stabilities). Thus it may be that the observations do not extend to high enough frequencies, although Figs 7 and 12 show there is little cospectral energy in this part of the spectrum. However, Deardorff (1972) has argued that departures from local isotropy might arise because horizontal velocity components tend to receive energy directly rather than via pressure gradients. Such an effect could be more noticeable in the higher wind conditions in which most of the present observations were made. A satisfactory explanation for these results is still outstanding and at present it is not clear whether this reflects an instrumental problem or a real effect. Better high frequency measurements are needed to clarify the situation.

Neither can the turbulent kinetic energy balance equation be used to discriminate between ϵ_u , ϵ_v or ϵ_w since the associated uncertainties are at least as great as the discrepancy in ϵ (eg Caughey & Wyngaard,

1979). Values of dimensionless turbulent kinetic energy dissipation are shown in Fig 16a. The curve represents the balance between the dissipation and the predicted shear production (using the non-dimensional velocity profile of Businger et al, 1971). All the values of ϵ scatter about this line. Fig 16b shows the corresponding non-dimensional dissipation rates of temperature and humidity fluctuations. In both cases, the values of dissipation are similar and fairly close to the estimated production term. This contrasts with some previous results (eg Leavitt & Paulson, 1975) in which the dimensionless temperature dissipation rates were almost an order of magnitude larger than the estimated production. However it is suspected that their data may have been contaminated (see Section 2).

8. Conclusions

The spectra and cospectra of velocity components measured alongwind agree very well with previous measurements made over the sea in similar conditions. They are also very similar to measurements made by Kaimal et al (1972) over land.

The humidity spectra agree equally well with previous results but it is clear that further work is required to establish the behaviour of temperature spectra over the sea. The present results show these to be clearly bimodal with a high frequency peak near $f = 0.6$. Such behaviour is supported by many of the previous results obtained over the sea, although the situation is further complicated by the possibility of salt contamination seriously affecting some measurements.

The degree of agreement found between the aircraft derived spectra and those made from fixed points implies that distortions of the latter arising from the use of Taylor's hypothesis are smaller than the uncertainties involved in making the measurements.

Although generally satisfactory for most of the turbulent variables, surface layer scaling was found to be least successful in reducing the wT -cospectra to a single curve. This, together with the behaviour of the temperature spectra, suggests that temperature fluctuations might only be successfully scaled in this manner at very low levels over the sea. This may be contrasted with the temperature spectra obtained over heated land surfaces which are very different from those presented here (in fact they resemble the present humidity spectra more closely). This presumably is a result of the very small air-sea temperature differences and the correspondingly small temperature fluctuation levels generated by subsequent buoyant mixing compared to the normal overland situation.

When sampled acrosswind, the spectra and cospectra (with w) of every parameter except v appear significantly different to the corresponding alongwind quantities. In each case there is a redistribution of energy from larger to smaller wavenumbers in going from acrosswind to alongwind data. This may be ascribed to an elongation of the u -eddies due to stretching by the mean shear (which is approximately parallel to the wind direction). Since the w , T and q fluctuations are correlated with those of u , so the w , T and q spectra are similarly affected. The overall result is that acrosswind spectra and cospectra are narrower, with significant energy being concentrated in only two decades (cf three in the the alongwind results). Spectral and cospectral peaks are also found at higher wavenumbers in acrosswind results although v -spectra are not distorted in this manner.

The major effect of increasing instability is to increase spectral densities at small wavenumbers, though this does not appreciably alter the shapes of the cospectra due to the very small proportion of the vertical velocity variance present in this part of the spectrum.

Good overall agreement was found between the calculated dissipation parameters and the expected production rates although a systematic bias was detected between the values of ϵ derived from different velocity spectra. It is not clear at present whether this is real or due to an instrumental defect. Further investigations into this problem are currently underway.

9. Acknowledgements

We would like to thank all those at MRF who contributed to this work, especially Mr Andrew Broughton who performed much of the tedious preliminary analysis.

References

- Bradshaw, P. 1978 Comments on "Horizontal velocity spectra in an unstable surface layer" J Atmos Sci 35 1765-1768
- Businger, J.A, Wyngaard, J.C 1971 Flux profile relationships in the atmospheric surface layer. J Atmos. Sci 28 181-189
- Izumi, Y, Bradley, E.F.
- Caughey, S.J, 1979 The turbulence kinetic energy budget and Wyngaard, J.C. in convective conditions. Quart J R Met Soc 105 231-240
- Deardorff, J.W. 1972 Numerical investigation of neutral and unstable planetary boundary layers. J Atmos Sci 29 91-115
- Donelan, M.A, and 1973 Spectra and fluxes in the boundary Miyake, M. layer of the trade-wind zone. J Atmos Sci 30 444-464
- Dyer, A.J. and Hicks, B.B. 1970 Flux gradient relationships in the constant flux layer. Quart. J.R. Met. Soc, 96, 715-721.
- Kaimal, J.C. 1978 Horizontal velocity spectra in an unstable surface layer. J Atmos Sci 35 18-24
- Kaimal, J.C, Wyngaard, J.C, 1972 Spectral characteristics of surface Izumi, Y, Cote, O.R. layer turbulence. Quart J R Met Soc 98 563-589
- Kaimal, J.C, Wyngaard, J.C, 1976 Turbulence structure in the convective Haugen, D.A, Cote, O.R, boundary layer. J Atmos Sci 33 2152-2169
- Izumi, Y, Caughey, S.J, and Readings, C.J.
- Leavitt, E. 1975 Spectral characteristics of surface layer turbulence over the tropical ocean. J Phys Oceanogr 5 157-163
- Leavitt, E and Paulson, C.A. 1975 Statistics of surface layer turbulence over the tropical ocean. J Phys Oceanogr 5 143-156
- LeMone, M.A. 1973 The structure and dynamics of horizontal roll vortices in the planetary boundary layer. J Atmos Sci 30 1077-1091
- Lenschow, D.H. 1970 Airplane measurements of planetary boundary layer structure. J Appl Met 9 874-884
- Nicholls, S. 1978 Measurements of turbulence by an instrumented aircraft in a convective atmospheric boundary layer over the sea. Quart. J. R Met. Soc., 104 653-676

- | | | |
|---|------|---|
| Nicholls, S. and
LeMone, M.A. | 1979 | The fair weather boundary layer in
GATE: The relationship of subcloud
fluxes and structure to the distribution
and enhancement of cumulus clouds.
Submitted to J. Atmos. Sci. |
| Nicholls, S. and
Readings, C J. | 1979 | Aircraft observations of the structure
of the lower boundary layer over the
sea. Accepted for publication by
Quart. J. R. Met Soc., |
| Panofsky, H. A. | 1978 | Matching in the convective boundary
layer. J. Atmos. Sci. <u>35</u> 272-276 |
| Phelps, G. T. and
Pond, S. | 1971 | Spectra of the temperature and humidity
fluctuations and of the fluxes of
moisture and sensible heat in the
marine boundary layer. J. Atmos Sci.
<u>28</u> 918-928 |
| Pond, S, Phelps, G.T,
Paquin, J.E. McBean, G.A.
and Stewart, R.W. | 1971 | Measurements of the turbulent fluxes
of momentum, moisture and sensible
heat over the ocean. J. Atmos. Sci. <u>28</u>
901-917 |
| Schmitt, K.F, Friehe, C.A.
and Gibson, C.H. | 1978 | Humidity sensitivity of atmospheric
temperature sensors by salt contamination.
J. Phys. Oceanogr. <u>8</u> 151-161 |
| Straka, J. Fiedler, F. and
Hinzpeter, H. | 1978 | Spectral transfer of turbulent energy
and temperature variance. Beitr. Phys.
Atmos. <u>51</u> 60-85 |
| Warner, J. | 1973 | Spectra of the temperature and humidity
fluctuations in the marine boundary
layer. Quart. J. R. Met. Soc., <u>99</u> 82-88 |
| Weiler, H.S. and
Burling, R.W. | 1967 | Direct measurements of stress and spectra
of turbulence in the boundary layer
over the sea. J. Atmos. Sci. <u>24</u> 652-664 |
| Zubkovskij, S. L. and
Koprov, B. M. | 1969 | Experimental investigation of the structure
of the turbulent heat and momentum fluxes
in the atmospheric surface layer.
Izv. Atmos. Oceanic Physics <u>5</u> 323-331 |

List of Figures

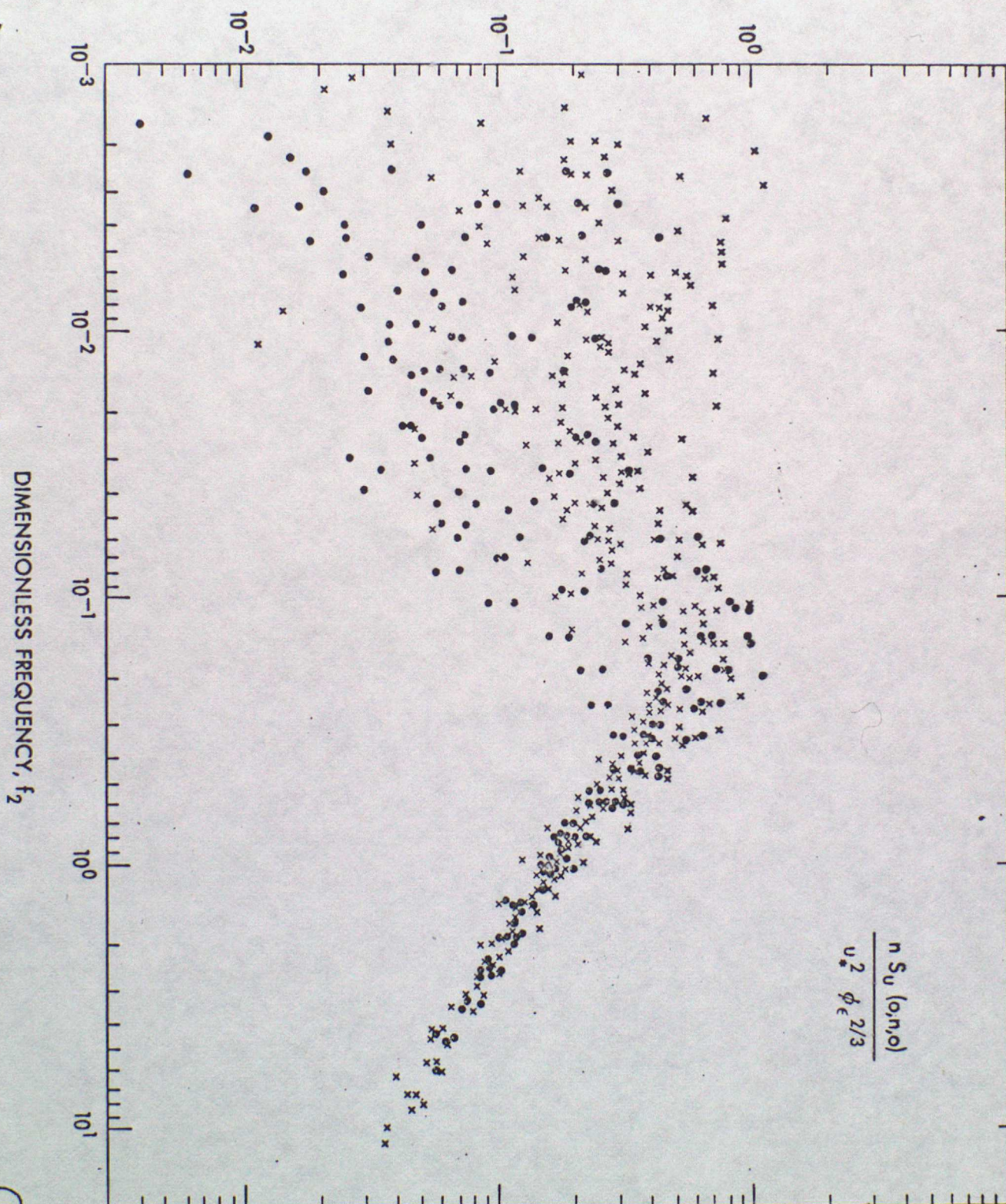
- Fig 1 Normalised acrosswind sampled u-spectra. x - class I (more unstable, $\hat{z} > 0.15$), • - class II (less unstable, $\hat{z} < 0.15$).
- Fig 2 Normalised alongwind sampled velocity spectra (class means plotted) ▲ - class I (more unstable, $\hat{z} > 0.15$), • - class II (less unstable, $\hat{z} < 0.15$). The curves represent corresponding results obtained over land by Kaimel et al (1972), see text for details.
- Fig 3 Location of w- spectral peaks as a function of height (both acrosswind and alongwind data included). • - class I (more unstable, $\hat{z} > 0.15$), x - class II (less unstable, $\hat{z} < 0.15$).
- Fig 4 Comparison of alongwind measured velocity spectra with previous measurements made over the sea. The shaded areas represent envelopes of results published by Pond et al (1971) and Leavitt (1975). Class mean values are plotted on (a) and (b), symbols as Fig 2, but individual points are plotted on (c) to show the scatter.
- Fig 5 (a) Normalised alongwind sampled temperature spectra, symbols as Fig 2. The curves represent the limits of the unstable Kansas data (Kaimel et al, 1972) obtained over land.
(b) Shapes of temperature spectra measured at low levels over the sea by: A, B - Phelps & Pond (1971), BOMEX and San Diego data respectively, C - Leavitt (1975) and D - Donelan & Miyake (1973).
- Fig 6 (a) Normalised alongwind sampled humidity spectra, symbols as Fig 2. The curves represent the limits of the unstable temperature spectra from Kaimel et al (1972) obtained over land.

(b) Comparison of alongwind sampled humidity spectra with previous measurements over the sea. The shaded area represents the envelope of results published by Phelps & Pond (1971) and Leavitt (1975). Symbols as Fig 2.

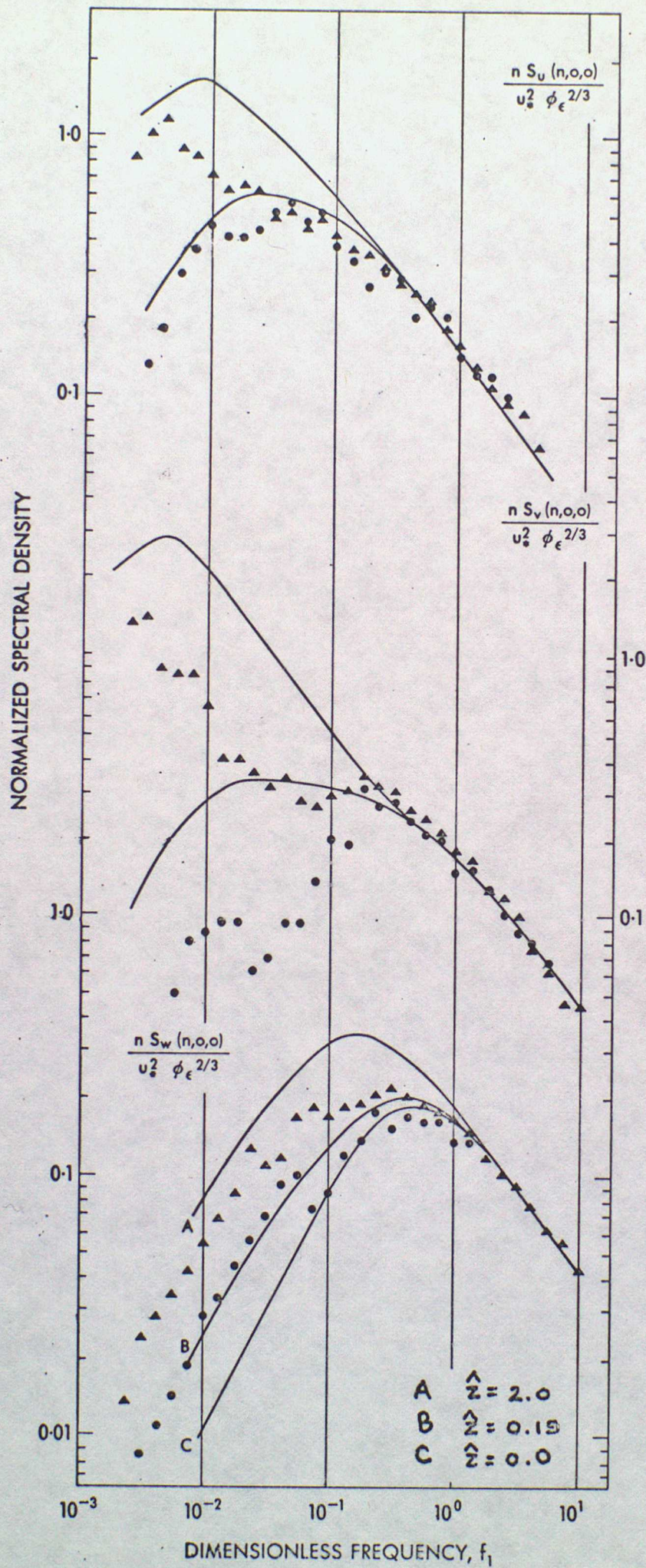
- Fig 7 Normalised alongwind sampled cospectra, classes I and II combined, denoted \bullet . Results from Leavitt (1975), denoted x, are included for comparison.
- Fig 8 Comparison of alongwind sampled cospectra with previous measurements over the sea. \bullet - mean of present measurements. The solid curves represent envelopes containing 95% of all individual cospectral estimates. The shaded regions represent the envelopes of results published by Pond et al (1971) and Leavitt (1975).
- Fig 9 Normalised acrosswind sampled velocity spectra. Symbols as Fig 2.
- Fig 10 Location of acrosswind sampled u- spectral peaks as a function of height. \bullet - class I data, \odot - class II data.
- Fig 11 Normalised acrosswind sampled temperature spectra (a) and humidity spectra (b). Symbols as Fig 2.
- Fig 12 Normalised acrosswind sampled cospectra, classes I and II combined, denoted \bullet . The full curves represent the envelopes containing 95% of the individual cospectral estimates. The dashed line on the wT - cospectrum defines the envelope for data where $z \leq 0.1 z_1$ ie the shaded portion contains only data from runs where $z > 0.1 z_1$. The dashed line on the uw- cospectrum defines the envelope for class II (less unstable) data ie the shaded portions contain only class I data (more unstable).

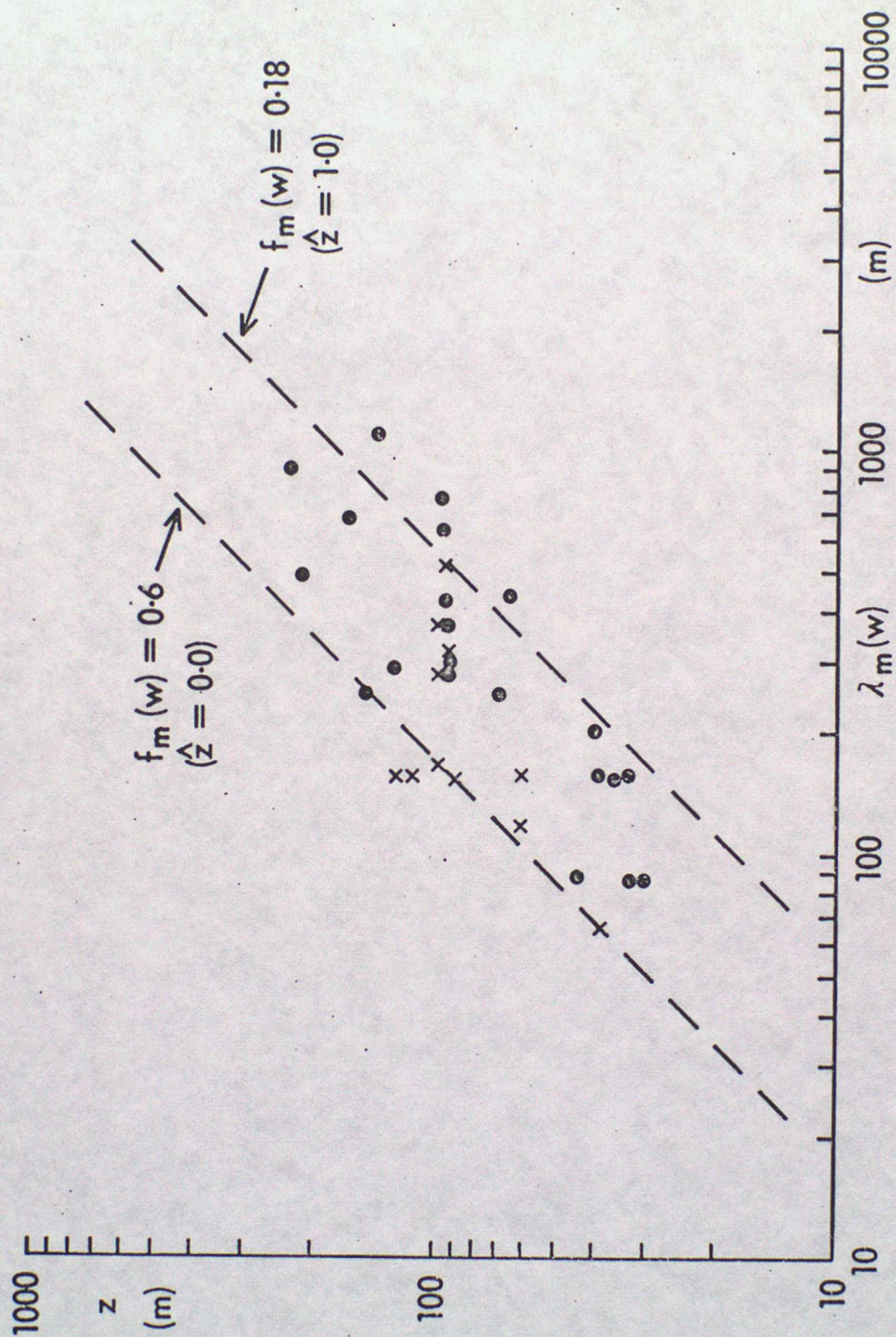
- Fig 13 Ratios of acrosswind to alongwind sampled spectral density as a function of dimensionless frequency. The full curve represents class I data, (more unstable), the dashed curve class II data (less unstable).
- Fig 14 Comparison of mean acrosswind sampled (full curves) and alongwind sampled (dashed curves) cospectra.
- Fig 15 Comparison of estimates of ϵ derived from different velocity components. \bullet - acrosswind sampling, \times - acrosswind sampling. The rightmost two sets of plots are displaced by one and two decades.
- Fig 16 Non dimensional dissipation estimates
- (a) Velocity fluctuations. \bullet - calculated using ϵ_u and ϵ_v
 \times - calculated using ϵ_w
- The full curve represents values of dissipation necessary to balance the shear production (assuming the non-dimensional velocity profile of Businger et al, (1971) ie $\phi_\epsilon = (1 + 15 \hat{z})^{-1/4}$)
- (b) Temperature (\times) and humidity (\bullet) fluctuations.
- The curve represents values of dissipation necessary to balance shear production (assuming the identical non-dimensional temperature and humidity profiles of Dyer & Hicks, 1970 ie $\phi_T, \phi_q = (1 + 16 \hat{z})^{-1/2}$)

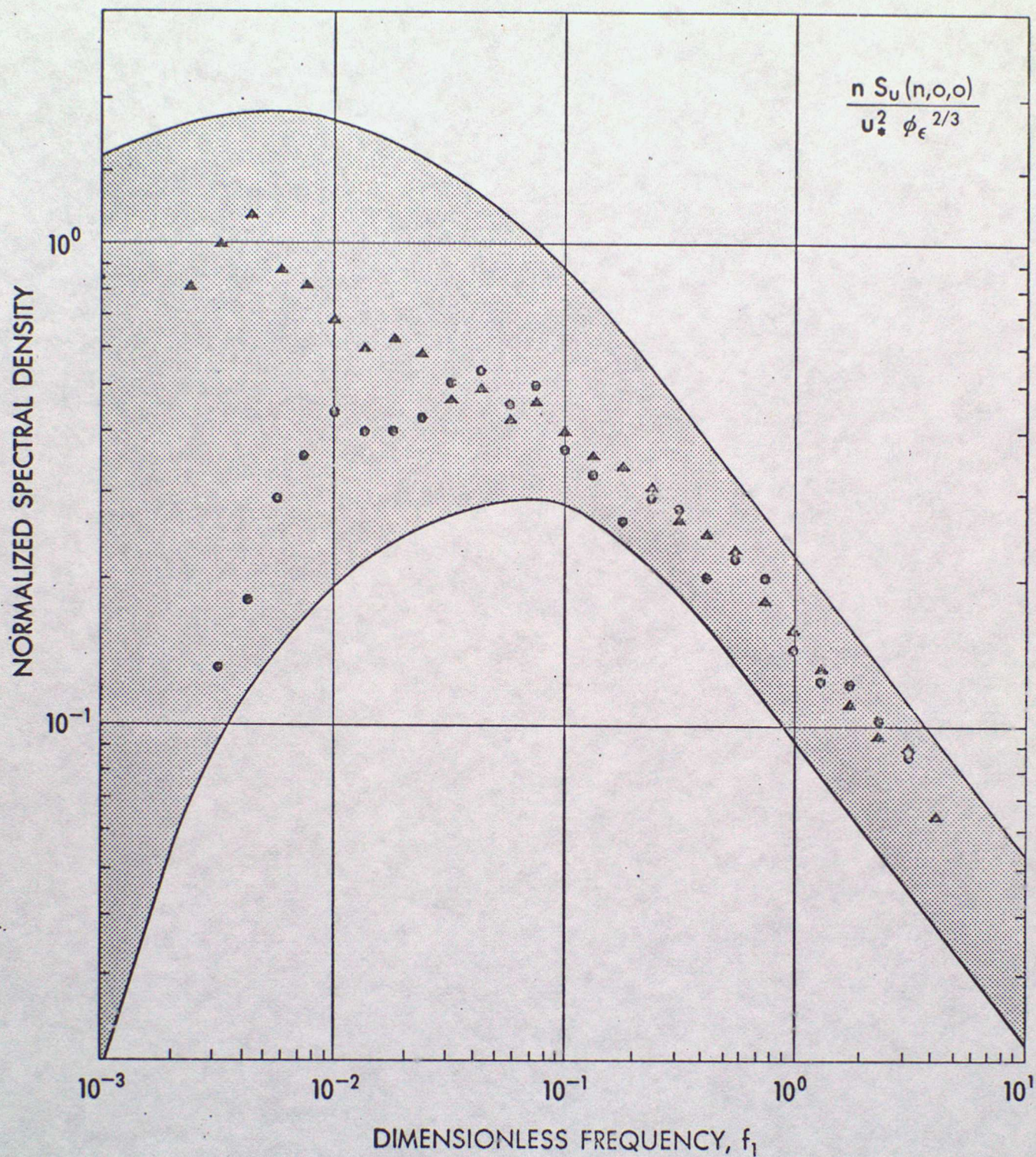
NORMALIZED SPECTRAL DENSITY

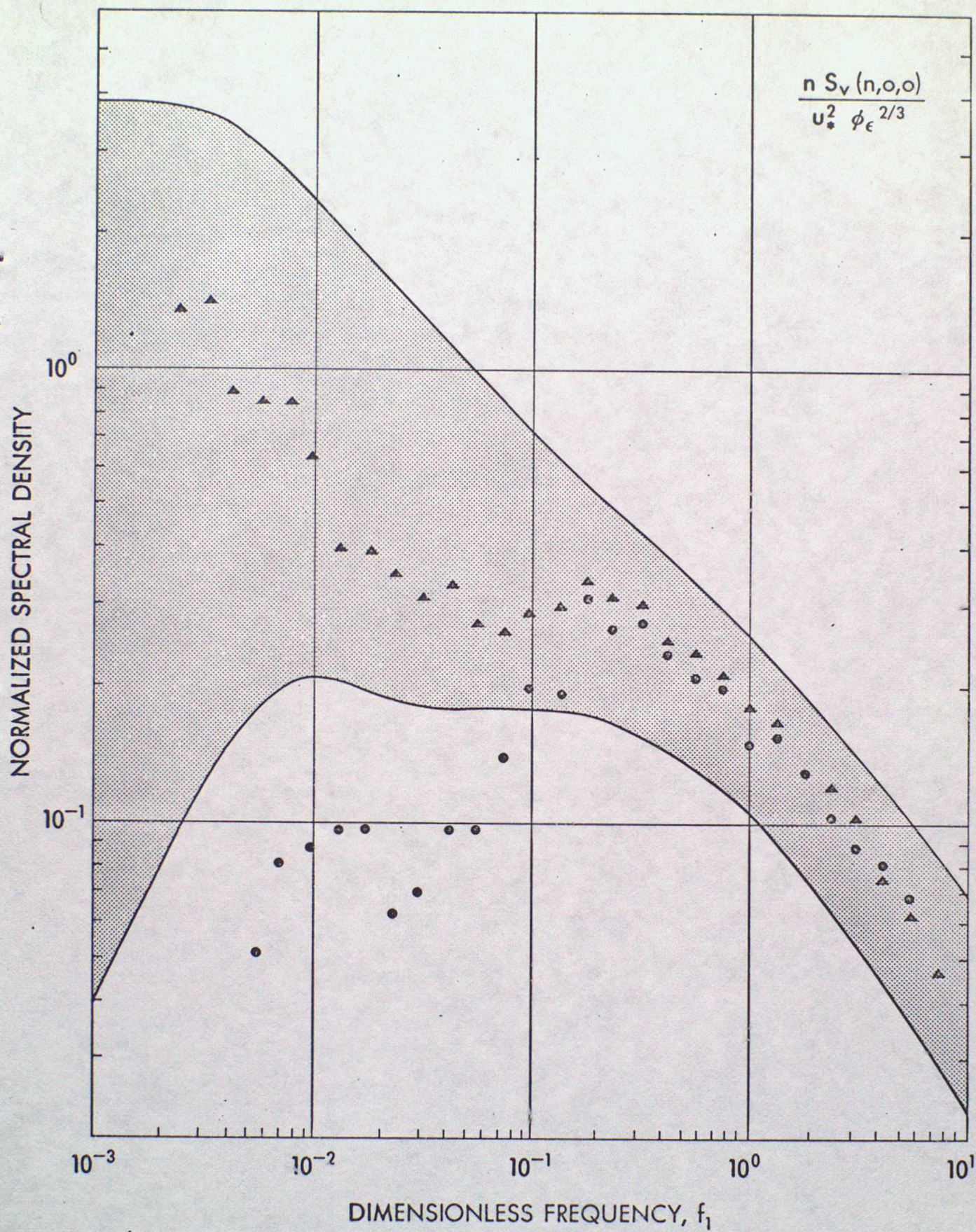


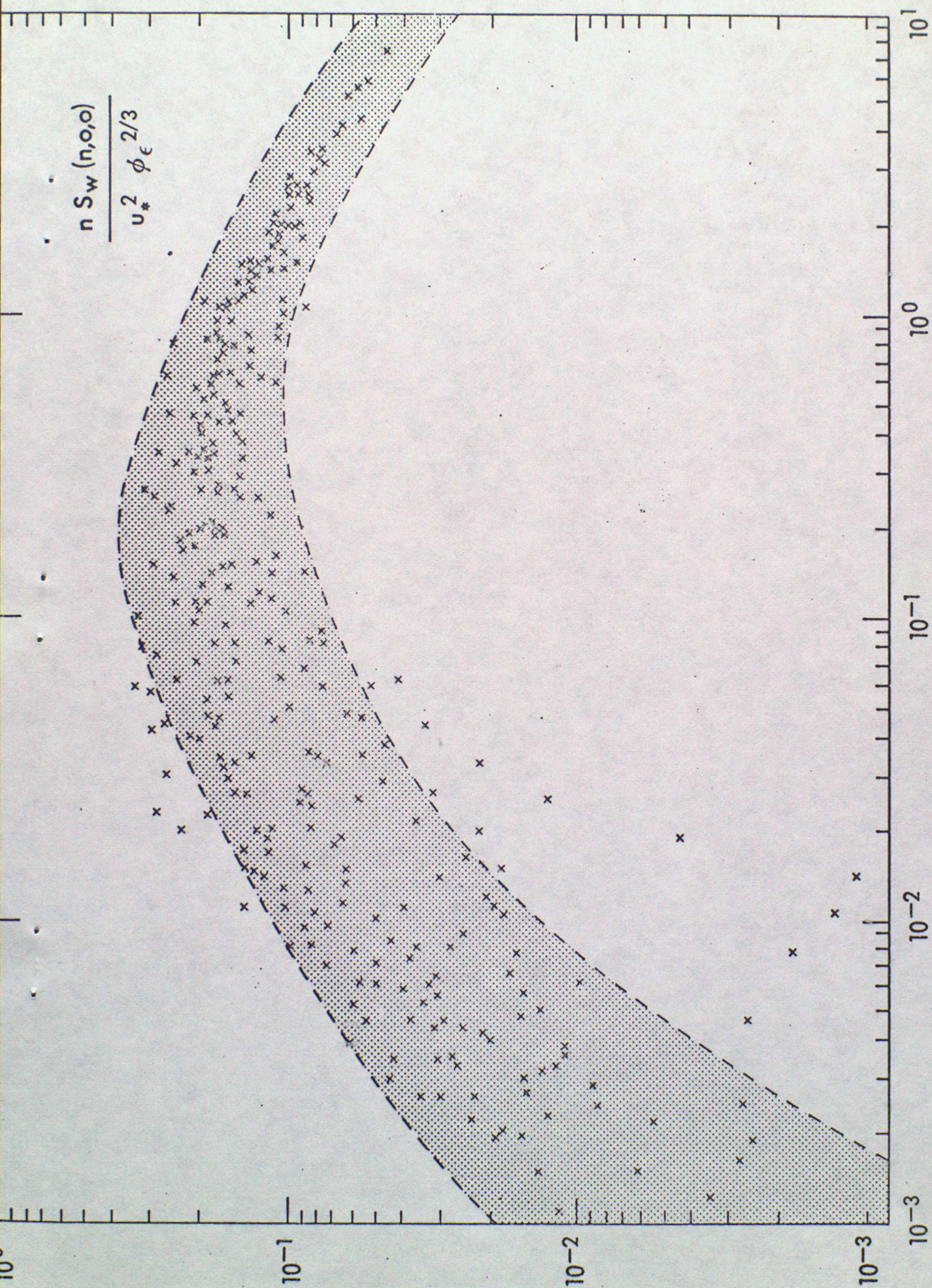
$$\frac{n S_u (o, n, o)}{u_*^2 \phi \epsilon^{2/3}}$$



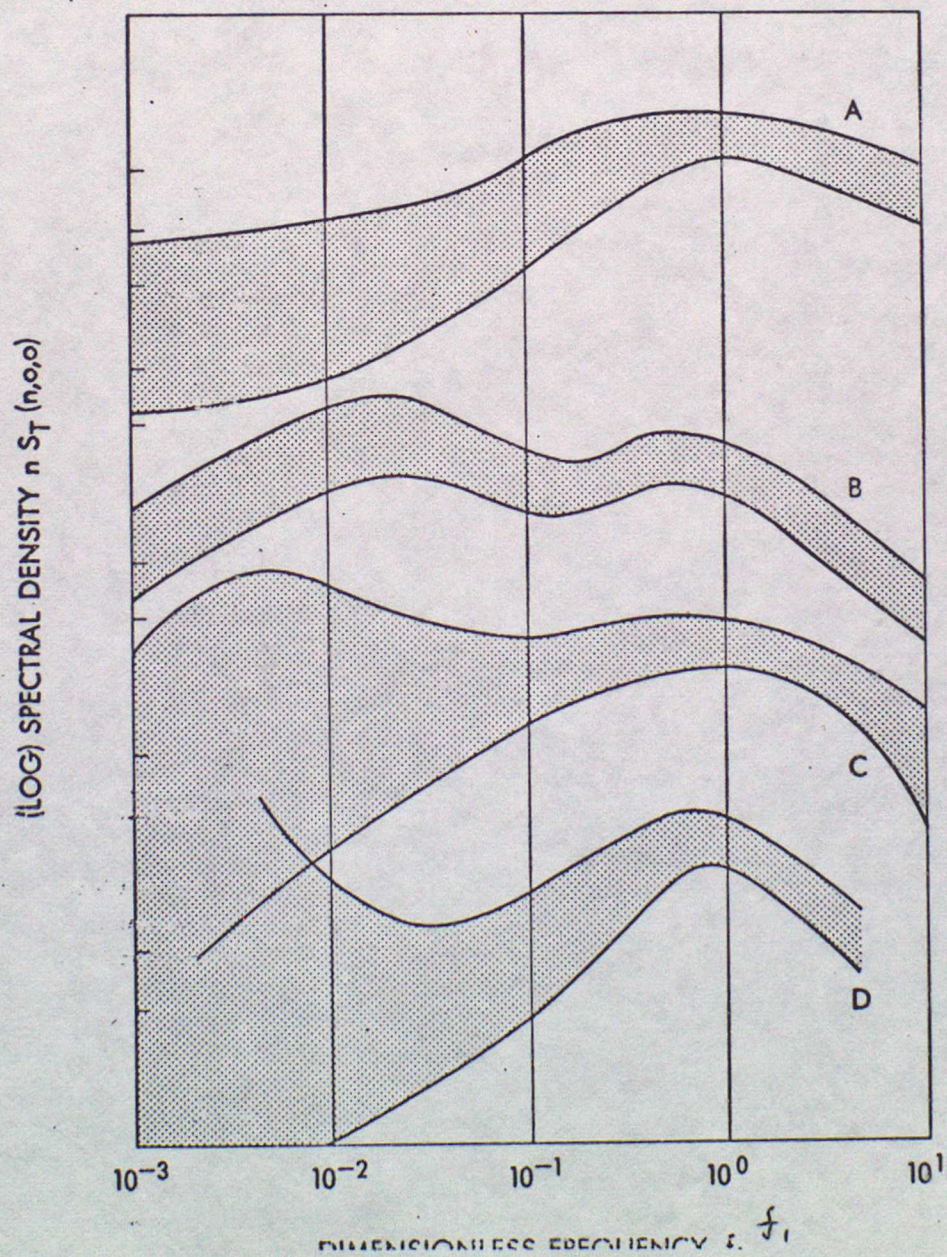
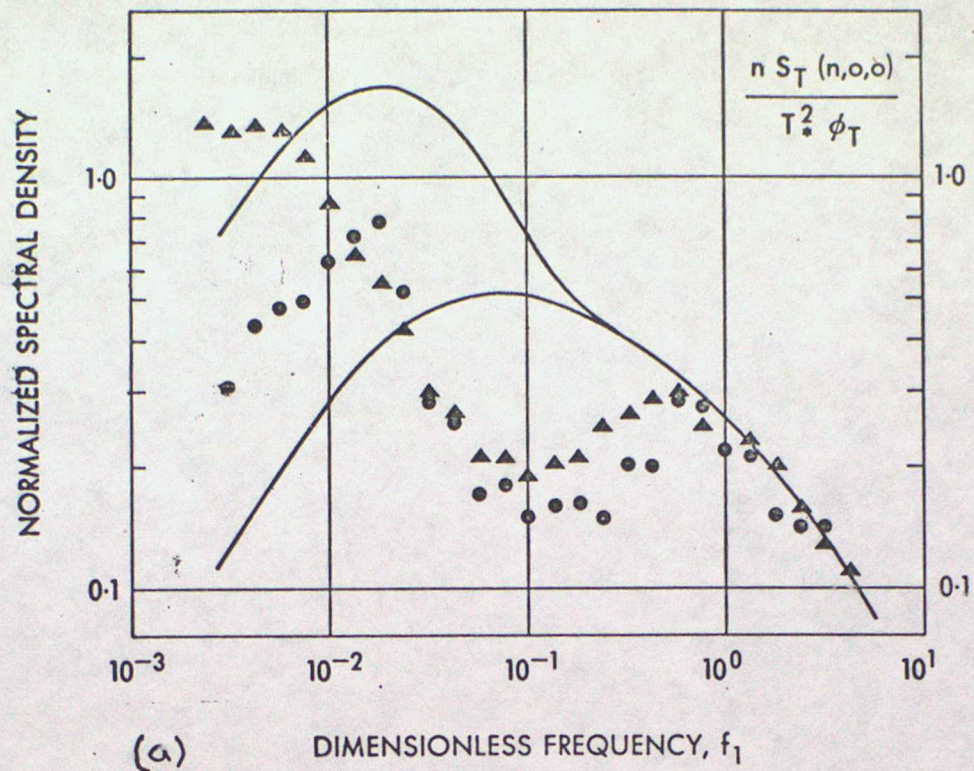


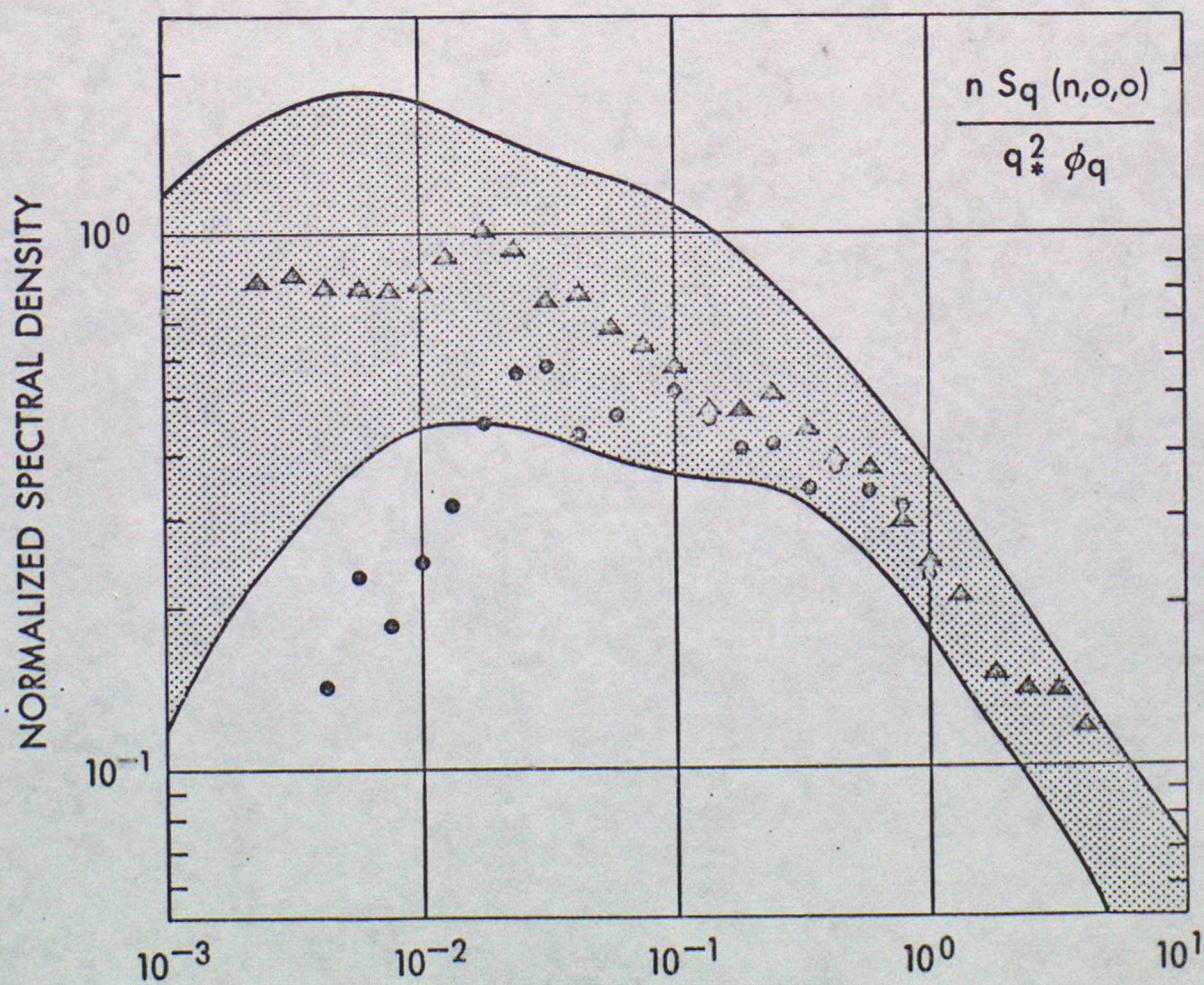
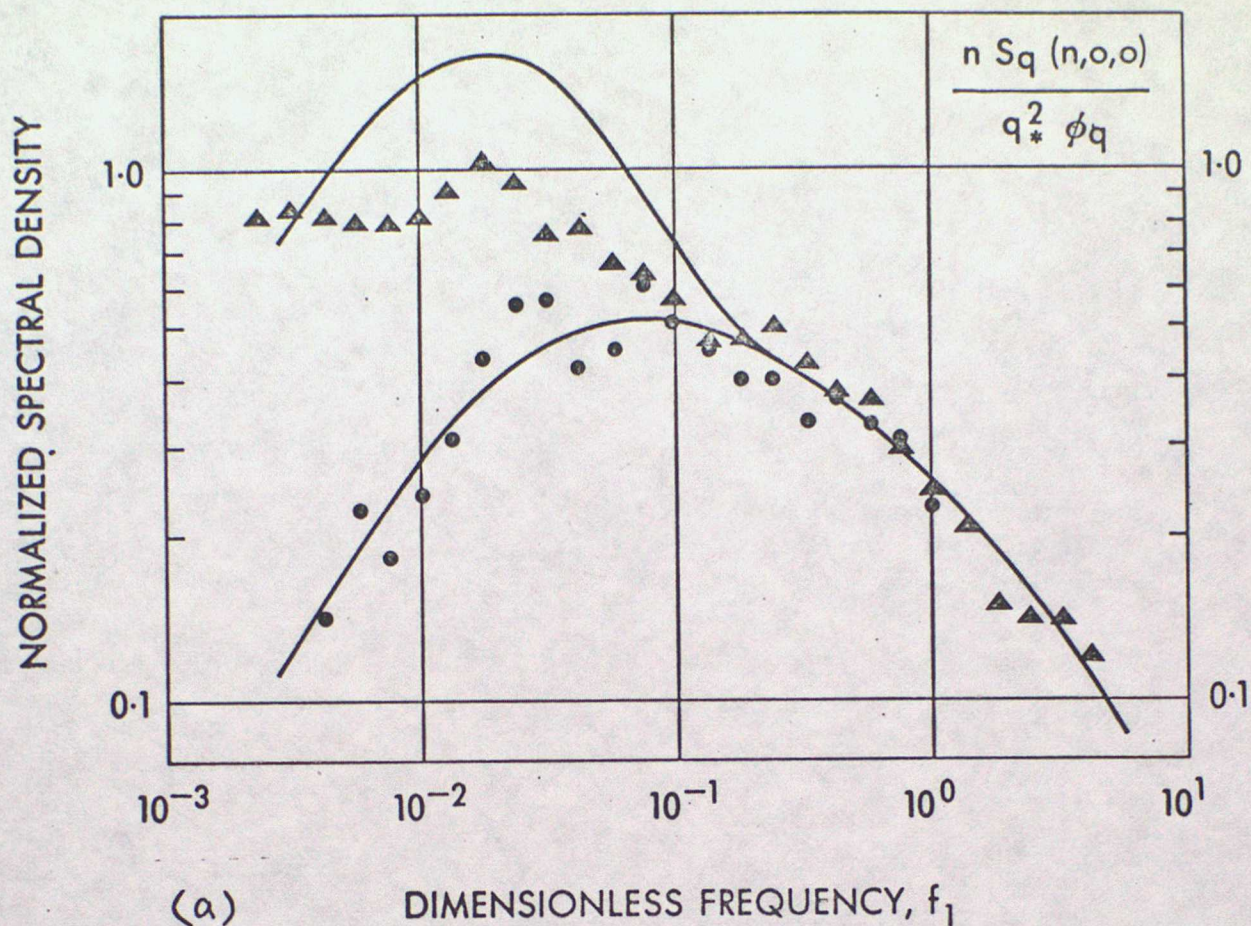


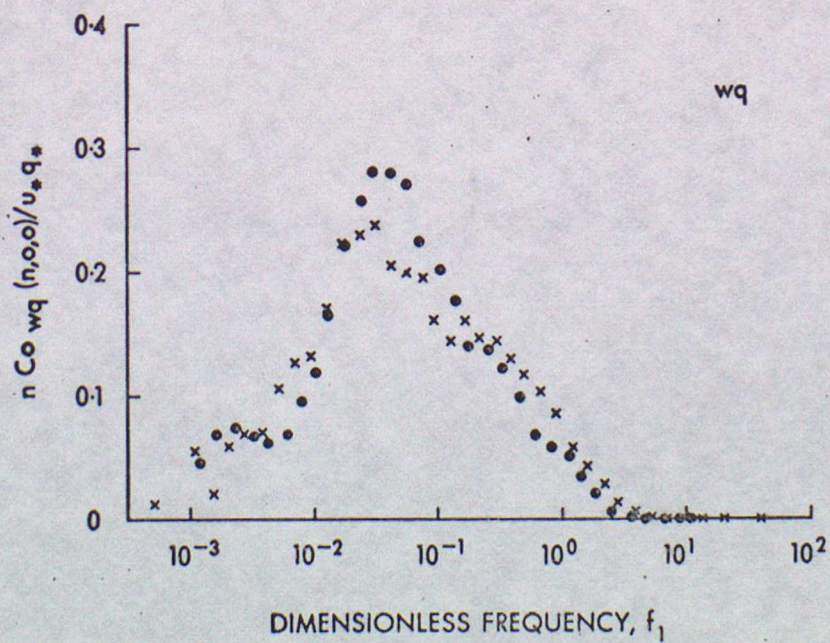
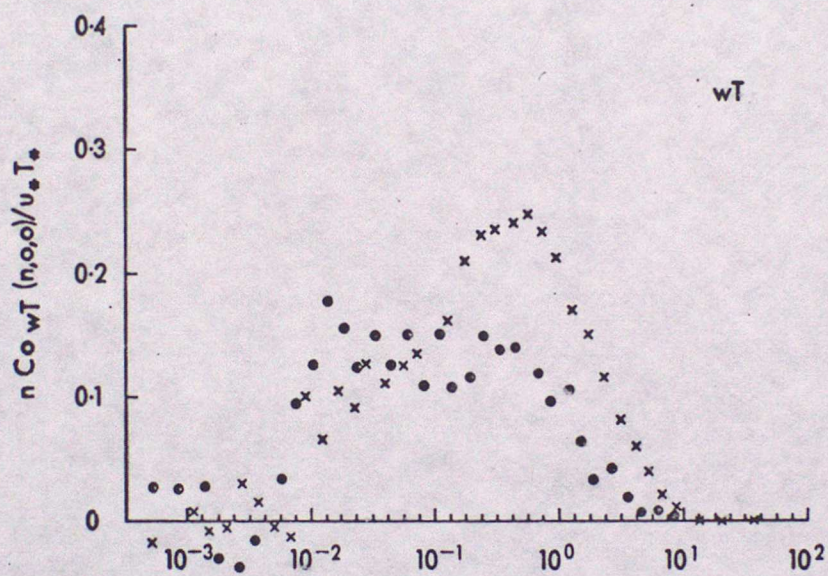
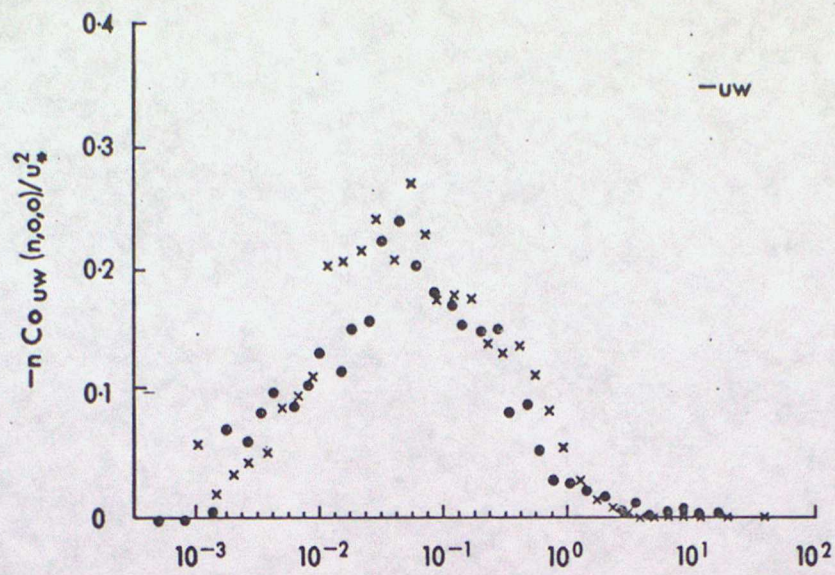


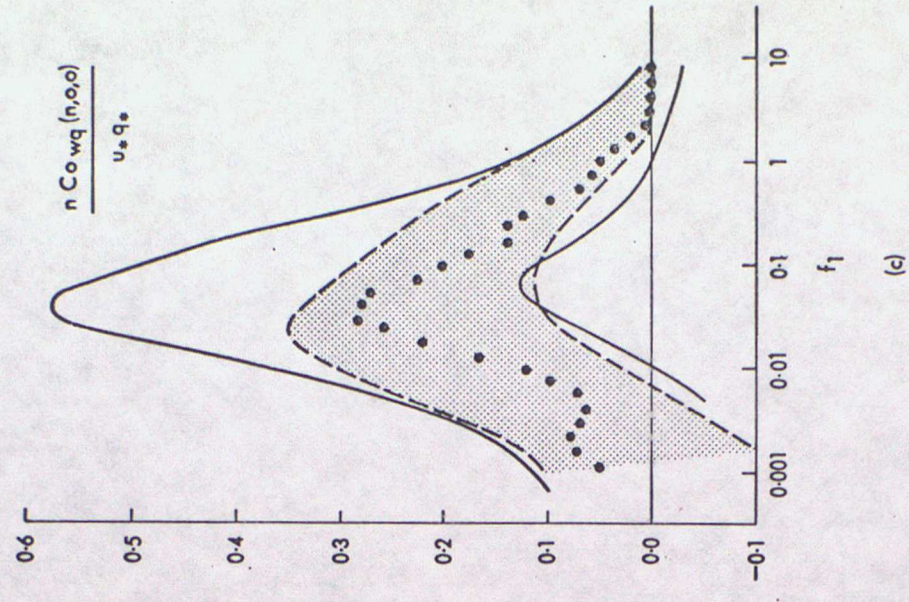
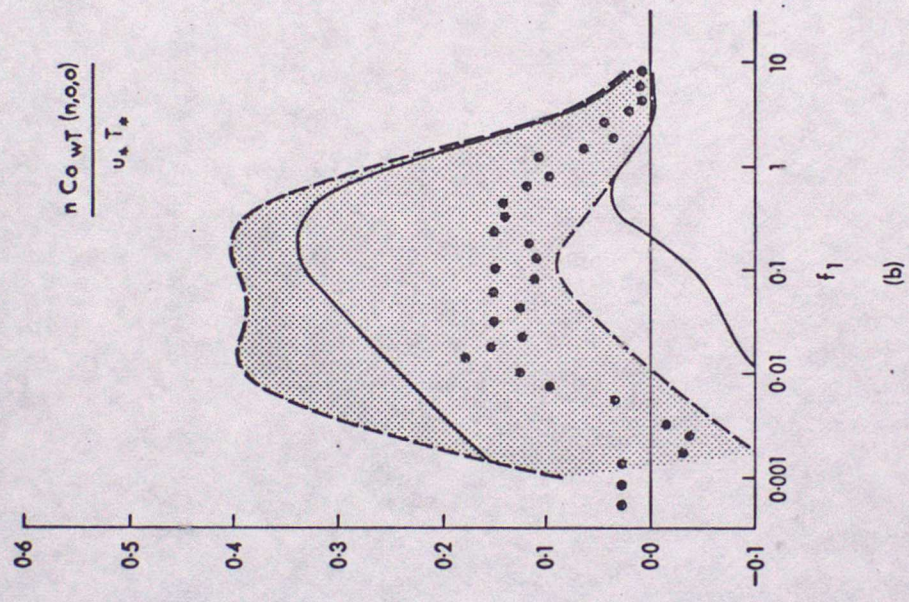
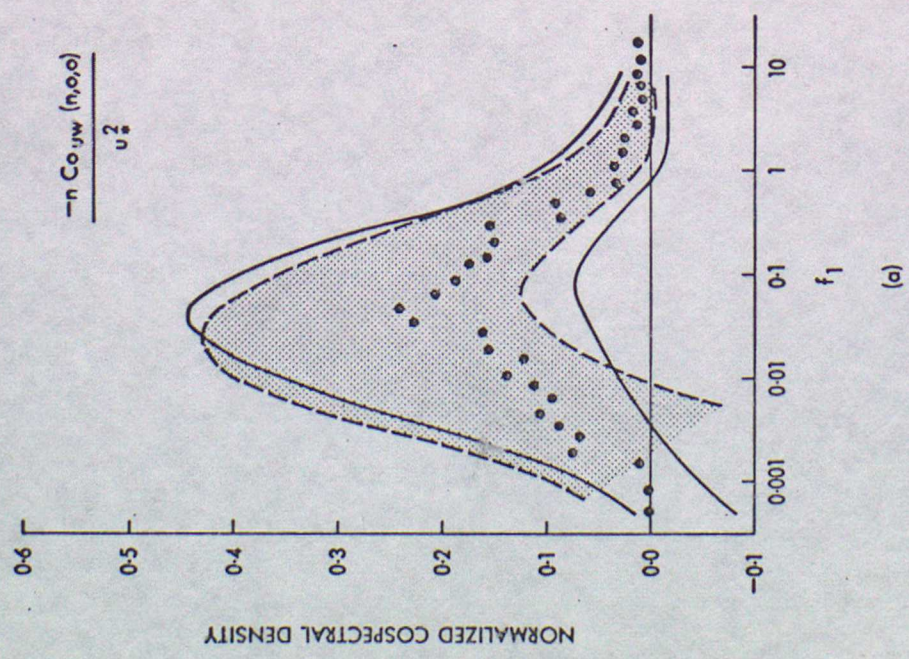


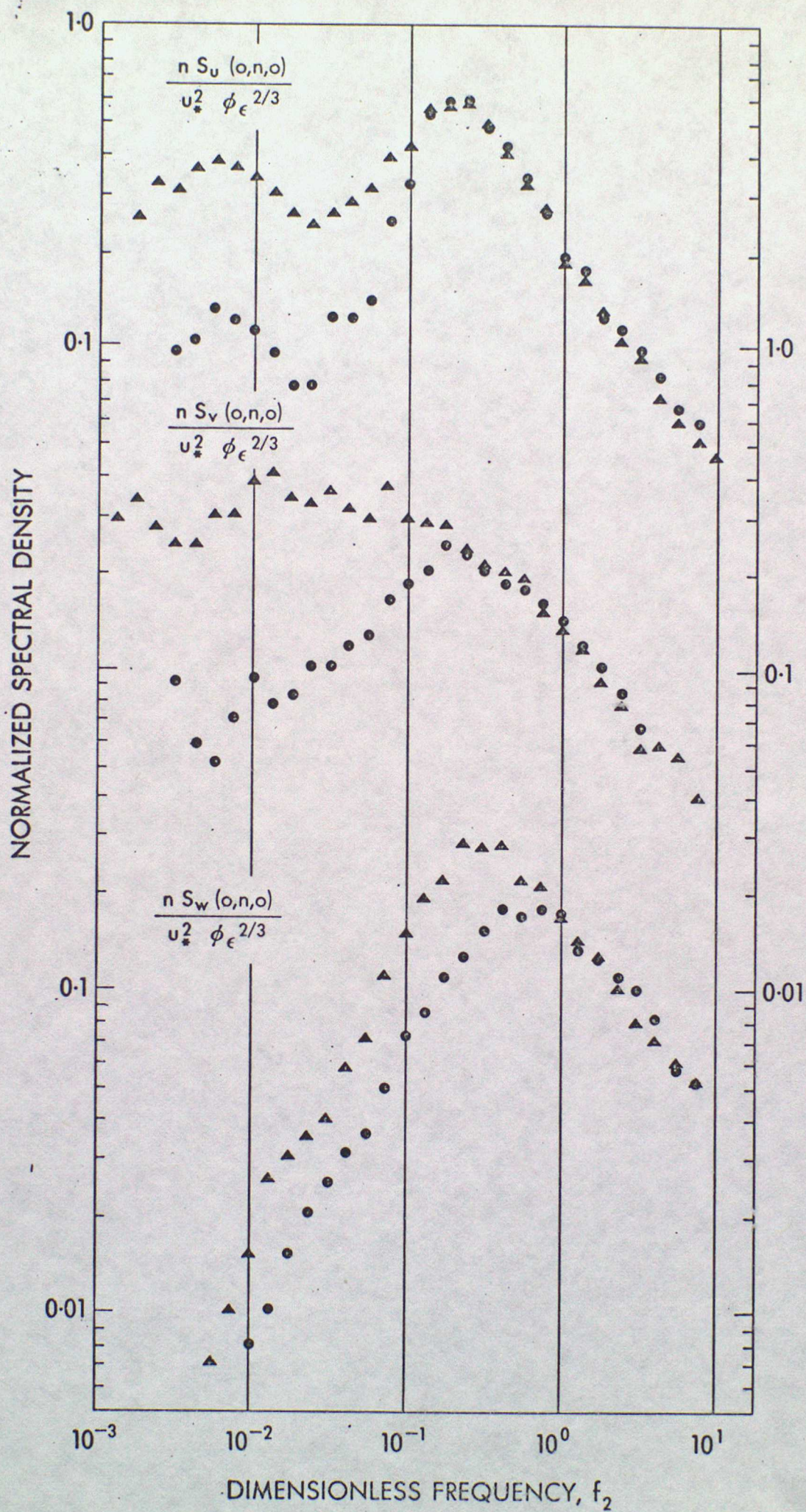
DIMENSIONLESS FREQUENCY, f_1

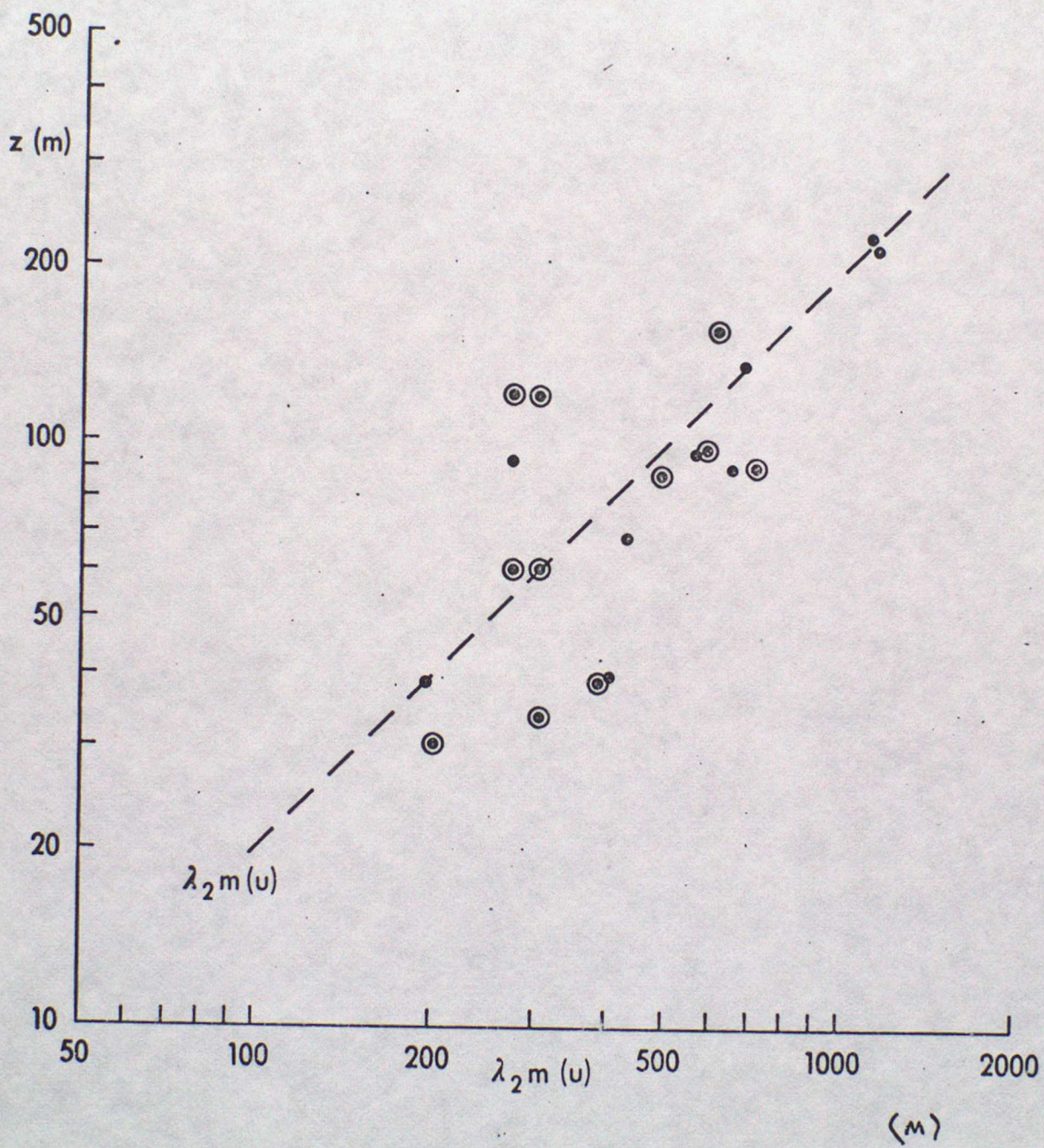


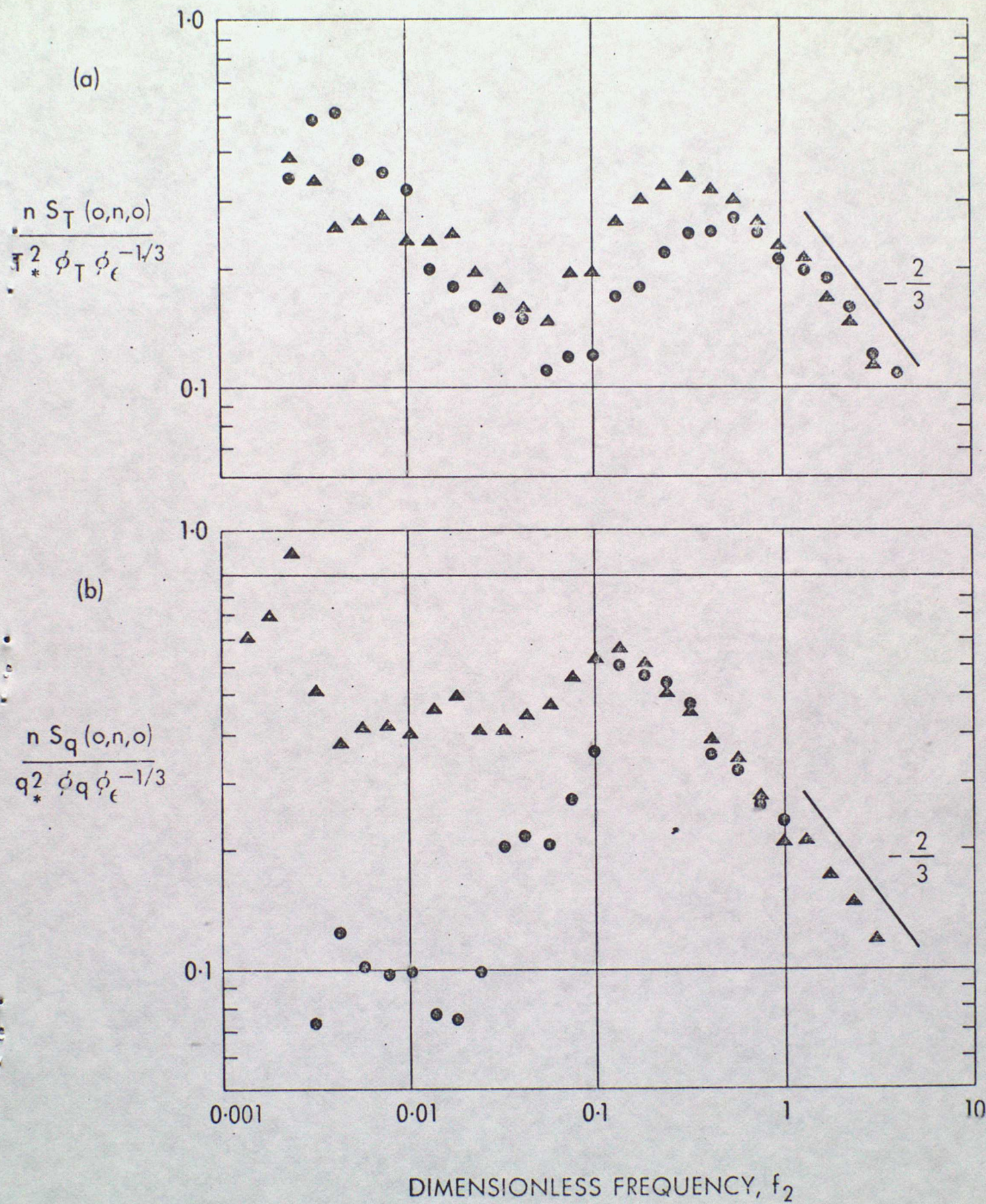


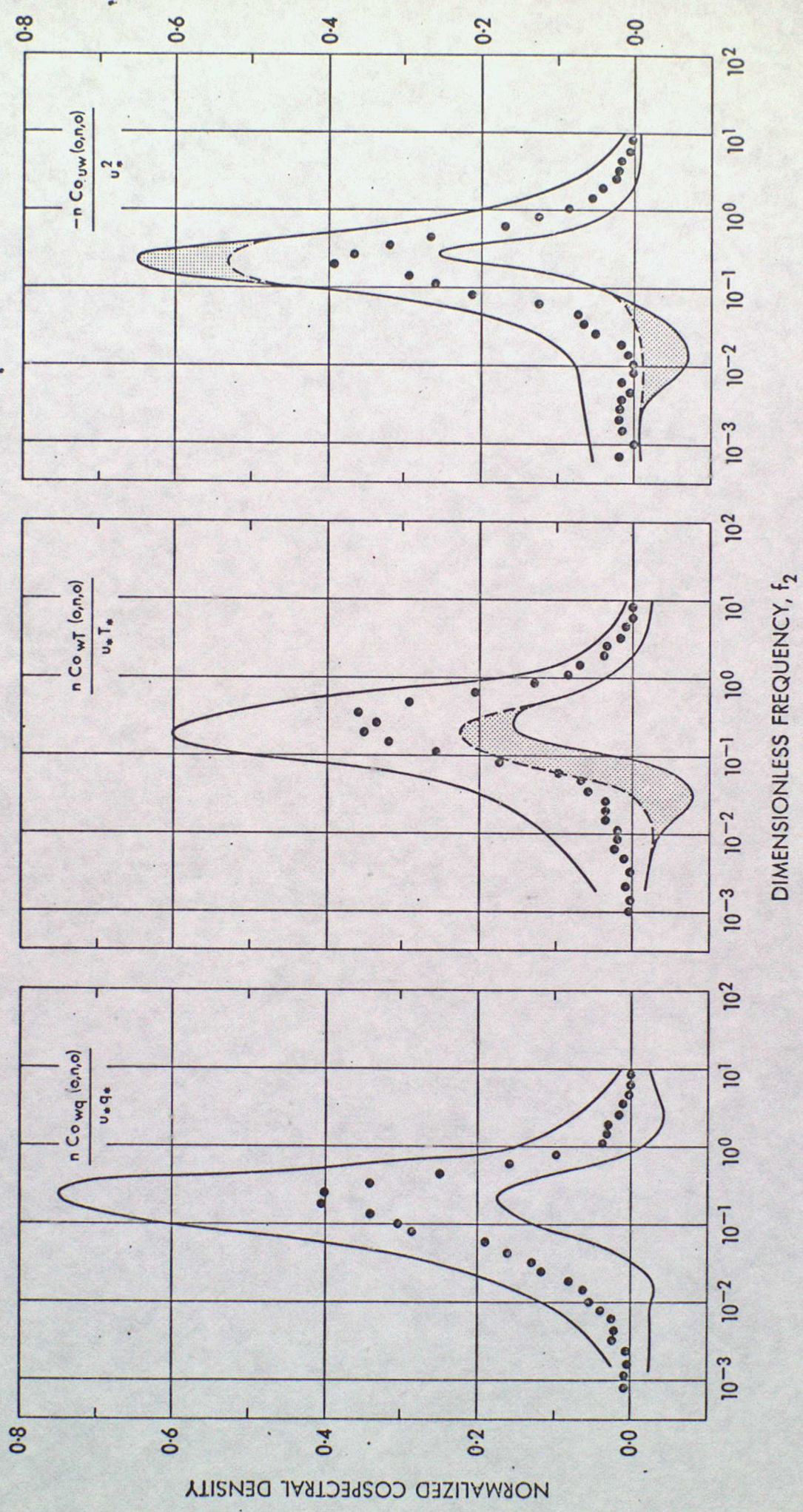












RATIO OF SPECTRAL DENSITIES — ACROSS WIND/ALONG WIND

